

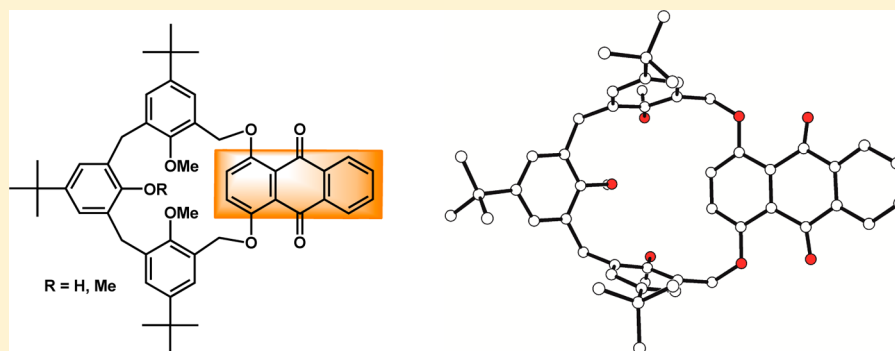
Synthesis of Macrocyclic Receptors with Intrinsic Fluorescence Featuring Quinizarin Moieties

M. Bürger,[†] F. Katzsch,[†] E. Brendler,[‡] and T. Gruber^{*,†}

[†]Institute of Organic Chemistry, Technische Universität Bergakademie Freiberg, Leipziger Strasse 29, Freiberg/Sachsen, Germany

[‡]Institute of Analytical Chemistry, Technische Universität Bergakademie Freiberg, Leipziger Strasse 29, Freiberg/Sachsen, Germany

S Supporting Information



ABSTRACT: An unprecedented class of macrocycles with intrinsic fluorescence consisting of phenolic trimers and quinizarin is developed. Though they are lacking strong hydrogen bonds as observed in calixarenes, the two examples introduced here each adopt a vase-like conformation with all four aromatic units pointing in one direction (*syn* orientation). This “cone” conformation has been confirmed by NMR spectroscopy, molecular modeling, and X-ray crystallography. The laminar, electron-rich fluorophore as part of the macrocycle allows additional contacts to enclosed guest molecules.

INTRODUCTION

Because of their high sensitivity, selectivity, and response time, fluorescence-based analytical techniques are extensively used in different fields of science. Respective sensors have been employed to detect a wide range of chemical and biochemical species as for example cations, anions, neutral molecules, biochemical analytes, and gases.¹ Thereby, the quality of the complexation equilibrium is indicated by a change in the intensity of the emitted light.² In many cases, the sensor-active materials used consist of a macrocycle connected to a pendant fluorophore. Much less studied are examples where the fluorophore is part of the recognition unit. The relevant literature very often includes condensed aromatic compounds such as naphthalene,³ anthracene,⁴ pyrene,⁵ fluorene,⁶ or related fluorophores.⁷

During our research on artificial hosts for methylammonium ions, we focused on cyclophanes as the macrocyclic recognition unit. They are a well-known class of supramolecular receptors, with the name being derived from their general constitution as “cyclic phenyl alkanes”.⁸ Especially [1_n]*m*-cyclophanes, so-called calixarenes, have attracted considerable attention over the last decades and are one of the best investigated cyclophane subfamilies,⁹ as they have a rather stable cavity and advantageous host/guest properties.¹⁰ Moreover, they are easily prepared and allow a wide range of derivatization reactions, which make them ideal candidates for the preparation of sensor-active compounds. In most cases, fluorophores were introduced at the upper or

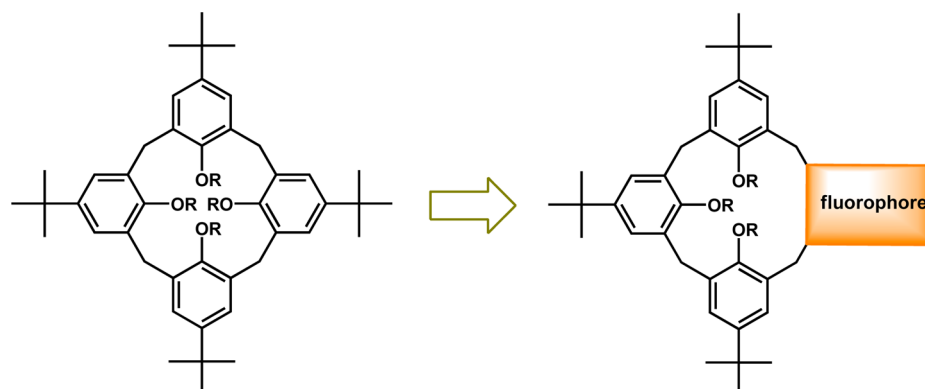
lower rim or in lateral positions,¹¹ hence bearing the responsive unit more or less in the periphery of the molecule. A rather less developed approach is the replacement of the phenolic units of a calixarene against fluorogenic moieties, which so far had only been shown for a complete exchange in the case of the calixnaphthalenes.¹² To the best of our knowledge, the replacement of only one of the phenolic units of a calixarene has not been explored yet, though the combination of conformational flexibility on the one hand and rigidity on the other seems a rather auspicious concept (Scheme 1). By inserting a condensed aromatic system, the resulting receptor is envisaged to enable better C–H⋯π and cation⋯π interactions with a methylammonium ion guest and at the same time allow an efficient quantification of host/guest interactions.

As a proof of concept to our approach, we advanced the synthesis of two rather simple representatives (1 and 2), featuring a *tert*-butyl group at the upper and methoxy units at the lower rim. As a fluorophore, we chose quinizarin (1,4-dihydroxyanthraquinone)^{13,14} delivering a receptor with a well-balanced combination of soft π-electrons and hard H-bond acceptors (C=O, OR), which is joined with putative functionalized phenolic trimers via ether bridges (Scheme 2).

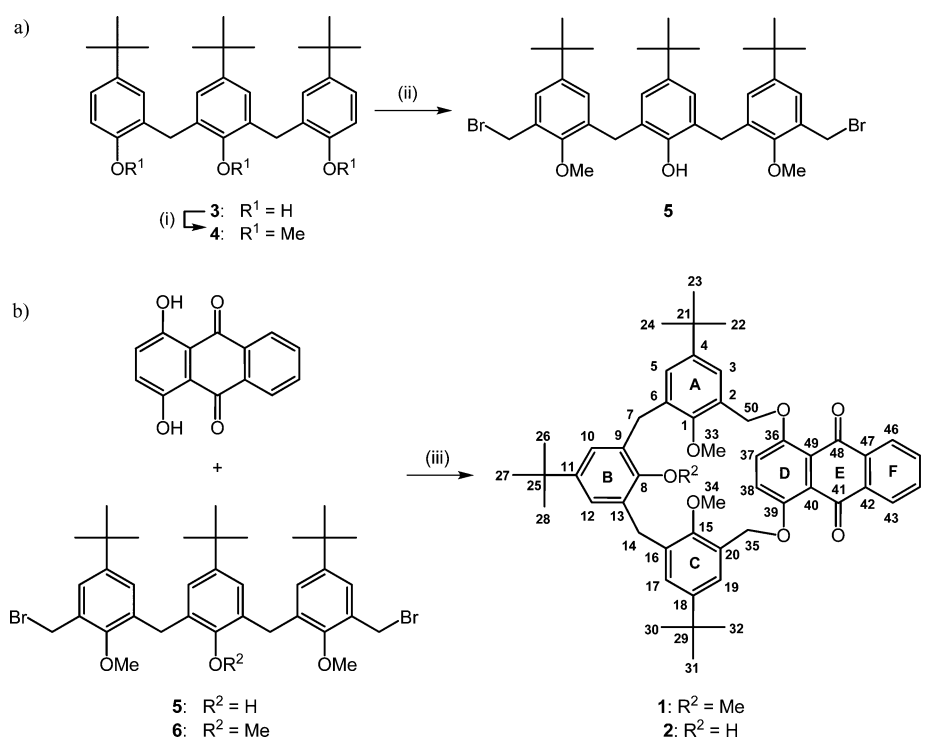
Received: January 30, 2015

Published: April 16, 2015

Scheme 1. Exchange of a Phenolic Unit of a Calix[4]arene against a Fluorophore Leads to a Receptor with Intrinsic Fluorescence

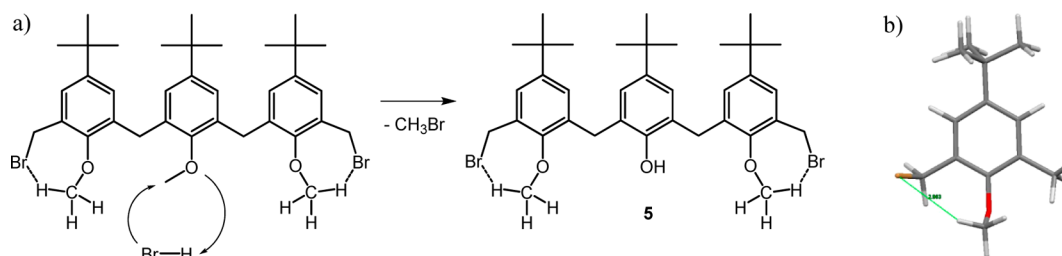


Scheme 2. (a) Synthesis of Monodemethylated Trimer 5. (b) Syntheses of Macrocycles 1 (58%) and 2 (18%)^a



^aReaction conditions: (i) 1. NaH, THF/DMF, 2. MeI; (ii) $(CH_2O)_m$, $ZnBr_2$, HBr/AcOH; (iii) K_2CO_3 , acetone.

Scheme 3. (a) Selective Ether Scission Induced by C–H \cdots Br Contacts of the Double Bisbromomethylated Intermediate in the Synthesis of 5. (b) The Energy-Minimized Structure Delivers C–H \cdots Br Distances of 2.92 and 2.96 Å, Respectively^a



^aOnly one of the bromomethylated anisole units is shown in detail.

RESULTS AND DISCUSSION

Syntheses of Fluorescophanes 1 and 2. The key step during the synthesis of the two title compounds is the formation of ether bridges between quinizarin and bisbromomethylated

trimers (5 or 6, respectively). As the preparation of 6¹⁵ has been achieved by a Blanc-analogue reaction on 3¹⁶ as described for a related compound,¹⁷ we want to focus here on the synthesis of 5. For similar partially methylated oligomers, two different

procedures have been applied so far: partial methylation of phenolic trimers with dimethyl sulfate¹⁸ on the one hand and isoaromatization of cyclohexanone derivatives¹⁹ on the other. We perceived another route via selective demethylation of a permethylated trimer as starting material. For that purpose, phenolic trimer **3** has been fully methylated in the first step to yield trimethoxy derivative **4**, which was subsequently treated with paraformaldehyde, zinc bromide, and hydrogen bromide in acetic acid (Scheme 2). In the first step of the reaction, two CH_2Br groups are introduced into the molecule, similar to a Blanc reaction. For the originating compound, we assume an interaction of the CH_2Br bromine atoms with the methoxy groups located at the same aromatic unit, withdrawing electron density from the respective ether oxygen atom. Suggested by molecular modeling, $\text{C}-\text{H}\cdots\text{Br}$ contacts are about 2.92 and 2.96 Å, respectively, which is shorter than the sum of the van der Waals radii of hydrogen and bromine (3.05 Å). Hence, the electrophilic attack of a proton, *viz.*, the first reaction step of an ether scission, will preferably occur at the central anisole moiety (Scheme 3).

With all particular trimeric fragments in hand, the synthesis of macrocycles **1** and **2** was implemented. Potassium carbonate has been applied as a base to deprotonate the two phenolic hydroxyl groups of quinizarin and facilitates a nucleophilic substitution analogously to a Williamson ether synthesis. As trimer **5** contains phenolic protons such as quinizarin, we examined the calculated $\text{p}K_{\text{a}}$ values: 7.5 for quinizarin and 10.3 for a monophenolic trimer²⁰ similar to **5**. Thus, quinizarin is expected to be deprotonated over 100 times faster than trimer **5**. To yield the smallest possible cycle during reaction, we used a high dilution apparatus²¹ applying the principle of Ziegler and Ruggli.²² With this concept, title compounds **1** and **2** were synthesized in moderate to good yields (58% and 18%, respectively). The somewhat lower yields in the cyclization step of **2** may be attributed to the phenolic hydrogen at the middle aromatic unit of trimer **5**: it is feasible to assume that it is also abstracted to a certain extent during the reaction delivering side products.

Conformational Studies. The given similarity of the target compounds with calixarenes suggests an analogue conformational behavior. As described for permethylated calix[4]arenes,²³ we expected rather complicated ^1H and ^{13}C NMR spectra for **1** and **2**. Surprisingly, both compounds delivered very clear NMR data (Figures S4–S7, Supporting Information, SI). In the ^{13}C NMR spectra the signals for $\text{Ar}-\text{CH}_2-\text{Ar}$ were found at 31.5 (**1**) and 30.3 ppm (**2**), suggesting a *syn* orientation for the three aromatic units involved.²⁴ Together with the ^1H NMR data for the aromatic protons, this points to a stable, highly symmetric conformation (cone) at room temperature. In both macrocycles, two constitutionally different methylene bridges can be identified, $\text{Ar}-\text{CH}_2\text{O}-\text{Ar}$ and $\text{Ar}-\text{CH}_2-\text{Ar}$, producing different chemical shifts. The OCH_2 group in **1** gives a broad singlet at 5.37 ppm; in **2** we found a broad doublet at 5.42 ppm. Whereas **2** delivers two broad singlets for the $\text{Ar}-\text{CH}_2-\text{Ar}$ protons at 3.43 and 4.30 ppm, the analogous signals in **1** are extremely broadened due to coalescence, underlying the signals of the OMe groups. These findings indicate unstable conformations at room temperature that may be explained from conformational conversions in **1** and **2**. These do not affect the chemical and magnetic environments of the aromatic nuclei, however, but do significantly for the methylene bridges.

The broad signals for the bridging methylene groups stimulated 1D and 2D NMR studies at lower temperatures, with typical spectra displayed in Figure 1. Both title molecules are

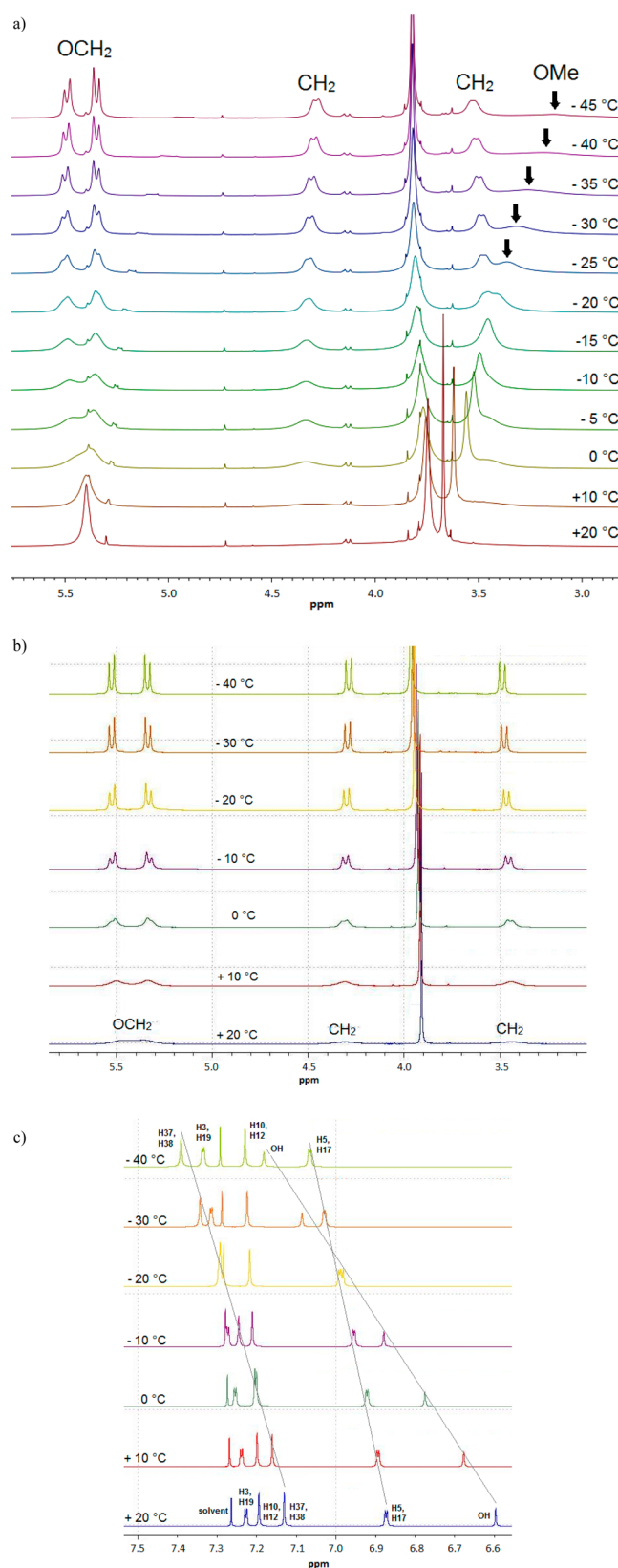


Figure 1. Details of the ^1H NMR spectra of **1** (a) and **2** (b, c) at different temperatures in CDCl_3 .

rather flexible, indicating a lower coalescence temperature than observed for the *tert*-butylcalix[4]arene ($52\text{ }^\circ\text{C}^{25}$ in CDCl_3). As the temperature had been lowered, the broad singlets of $\text{Ar}-\text{CH}_2\text{O}-\text{Ar}$ split into a pair of doublets with 2J coupling constants

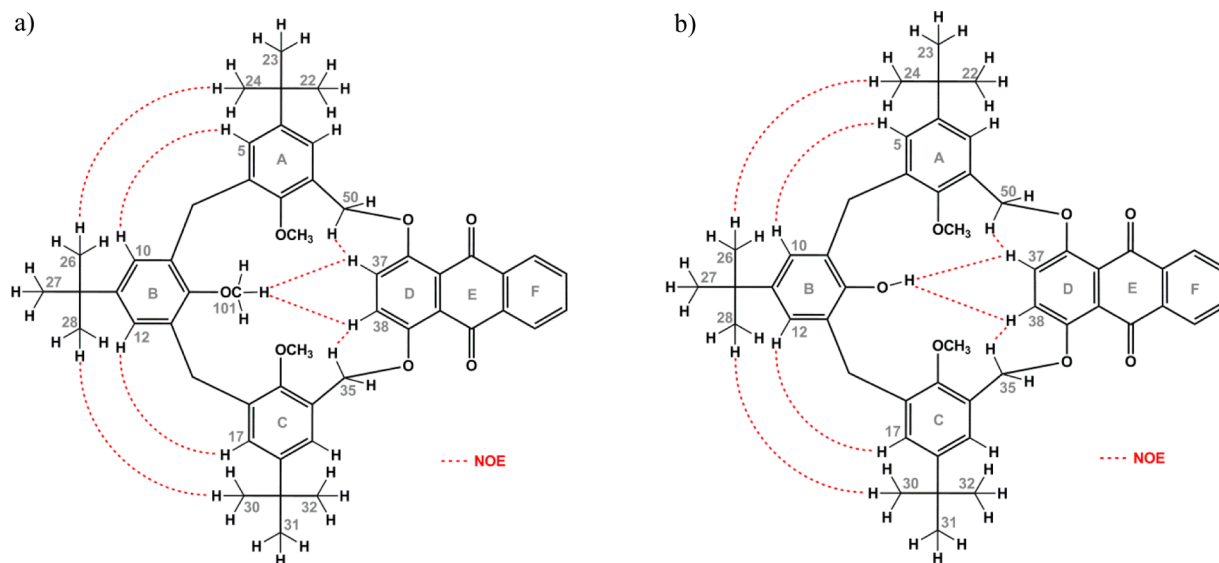


Figure 2. Observed NOEs, indicated by dotted lines, for title compounds **1** (a) and **2** (b) in CDCl_3 at 20°C . No NOE contacts indicating conformations other than a cone were observed for either cyclophane.

of 15 Hz for **1** and **2**. Lacking of strong hydrogen acceptors, **1** shows a higher flexibility than **2** as also proven by the behavior of the $\text{Ar}-\text{CH}_2-\text{Ar}$ units: even at -40°C the conformational conversion in compound **1** does not allow the complete resolution of the couplings between the axial (*endo*) and equatorial (*exo*) protons ($^2J = 15$ Hz, each). Interestingly, in **2** the aromatic protons H3 (H19) and H5 (H17) of ring A (C), H37 (H38) at quinizarin ring D, and the hydroxyl proton are subjected to a considerable downfield shift during cooling. We attribute this to a decreasing thermal dynamic mobility of the pending hydroxyl and methoxy groups. It is feasible to assume that at the same time hydrogen bonding of H37 (H38) and the hydroxyl proton with the two oxygen atoms of the methoxy groups is strengthened. Hence, the aromatic protons H3 (H19) and H5 (H17) of ring A (C) are turning slightly away from the shielding cyclophane cavity. For the aromatic region of cycle **1** we only found insignificant shifts during cooling for H5 (H17), H10 (H12), and H37 (H38), though not for H3 (H19). Noteworthy, all aromatic signals exhibit broadening as the temperature was lowered, suggesting dynamic conformational exchange (Figure S8, SI).

As the pending methoxy groups are not directly involved in the coalescence, we anticipated sharp ^1H NMR signals for OCH_3 at room temperature, which proved to be true for cycle **2**. A respective singlet at 3.91 ppm for the OCH_3 groups indicates a more or less rigid cavity, supposedly fixed by strong $\text{O}-\text{H}\cdots\text{O}$ hydrogen bonds between the hydroxyl and the methoxy moieties. In **1** only the central methoxy group delivered a sharp singlet (3.67 ppm). However, the methyl groups of the two outer anisole units in **1** gave a rather broad singlet at 3.72 ppm. Obviously, the methoxy group at ring B is much more flexible at room temperature than the ones at ring A and C. The OCH_3 signal on the B ring was broadened and upfield-shifted (3.67 ppm \rightarrow 3.18 ppm) with the temperature lowering; this is typical for methoxy groups pointing into a cyclophane cavity.²⁶ As the conformation of the macrocyclic backbone is getting more stable while cooling to -40°C , the free rotation of methoxy group B is obstructed and slowed down to the NMR time scale. Owing to the obstructed rotation of the methoxy group(s), a rather low

resolution of the two doublets of $\text{Ar}-\text{CH}_2-\text{Ar}$ and the broadened OCH_3 singlet(s) even at -45°C is observed.

In principle, the anthraquinone units in the target molecules can adopt two positions: opposite the anisole moieties or away from them. To solve this issue, we performed 2D NOESY spectra of **1** and **2** at room temperature and -40°C (for **2**), elucidating the proximity of the different aromatic units of the molecule (Figure 2 and Figures S9 and S10, SI). For both macrocycles, we found NOEs between the aromatic protons H5/H10 and H12/H17 (**1**: 6.81/7.25 ppm; **2**: 6.89/7.19 ppm) indicating that all three aromatic moieties are in a *syn* conformation even at room temperature. This is also confirmed by interactions between the *tert*-butyl groups of rings A and C with the one of ring B (0.86/1.38 ppm for **1** and 0.88/1.34 ppm for **2**). The arrangement of the anthraquinone unit has been determined from interactions of quinizarin ring D (H37) with other regions of the molecule. For **1**, we observed NOEs between H37 and OCH_2 (6.78/5.37) as well as H37 to the methoxy group of ring B (6.78/3.63), which is only possible when all four aromatic units are in a *syn* arrangement, i.e., the macrocycle is in a cone conformation. The same conformation can be assumed in **2**, as its OH group is involved in dipolar interactions with H37/38 of ring D (6.62/7.13 ppm). At -40°C we were able to identify additional NOEs between H5 (H17)/H10 (H12) and the axial proton of the adjacent methylene bridges.

Molecular Modeling Studies. For supplementing the spectroscopy studies on the conformational properties of both macrocycles, we performed molecular modeling studies. With exception of a strong hydrogen bond between the phenolic OH and a neighboring methoxy moiety in **2**, no strong hydrogen bonds have been found. However, the quinizarin units in both target molecules are engaged into inverse-bifurcated $\text{C}-\text{H}\cdots\text{O}$ contacts (Figure 3), stabilizing the cone conformation of both cycles (Figure S1, SI).

Single X-ray Studies. To verify the results from the spectroscopic and the modeling studies, we investigated the molecular structure of the title compounds by X-ray crystallography. When crystallized from acetonitrile/chloroform and acetonitrile, respectively, compounds **1** and **2** gave the inclusion compounds **1a** [**1**:acetonitrile-chloroform (2:2:1)] and **2a** [2:

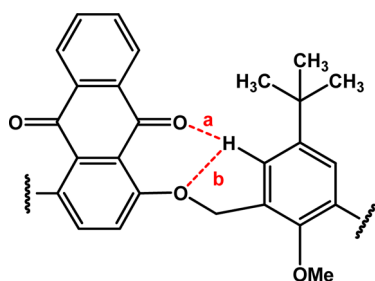


Figure 3. Common H-bonding motif in **1** and **2** found by molecular modeling studies. **1**: $a = 2.721 \text{ \AA}$, 2.692 \AA ; $b = 2.729 \text{ \AA}$, 2.752 \AA ; **2**: $a = 2.543 \text{ \AA}$, 2.638 \AA ; $b = 2.583 \text{ \AA}$, 2.630 \AA .

acetonitrile (3:1)] (Table S1, SI). Perspective views of the asymmetric units and the crystal packings are displayed in Figures 4–7. For the description of the molecular conformations of the host compounds, we determined the inclination of the aromatic rings with respect to the mean plane of the four methylene groups of the molecules. Complementarily, the dihedral angles between pairs of opposite arene rings have been designated. These parameters together with structural details on the quinizarin units are summarized in Table 1; specifics on hydrogen bonds and other contacts are listed in Table S2 (SI).

Table 1. Selected conformational parameters of compounds **1a** and **2a**

	interplanar angles (deg) ^a		
	1a (1)	1a (2)	2a
mpla A/mpla C	41.9	35.9	33.4
mpla B/mpla Q ^b	79.2	68.5	76.4
mpla M ^c /mpla A	73.1	78.1	79.5
mpla M/mpla B	41.8	36.5	51.4
mpla M/mpla C	72.8	74.0	72.4
mpla M/mpla Q	37.7	32.1	52.3
mpla D/mpla F	11.0	11.0	8.6
ACN/mpla M	45.0	40.1	46.8

^aAromatic rings: ring A: C1...C6; ring B: C8...C13; ring C: C15...C20; ring D: C36...C49; ring F: C42...C47. ^bBest plane through atoms of the quinizarin unit: C36...C49. ^cBest plane through the carbon atoms of the methylene bridges C7, C14, C35, C50.

Crystallization of trimethoxy receptor **1** from acetonitrile/chloroform (1:1) gives inclusion compound **1a** in the monoclinic space group $C2/c$. The asymmetric unit consists of two crystallographically independent host molecules, two acetonitrile (ACN) molecules, and one molecule of chloroform. The CH_3CN guests are incorporated within the host cavities, the chloroform is situated clathrate-like in lattice voids. (In total, the

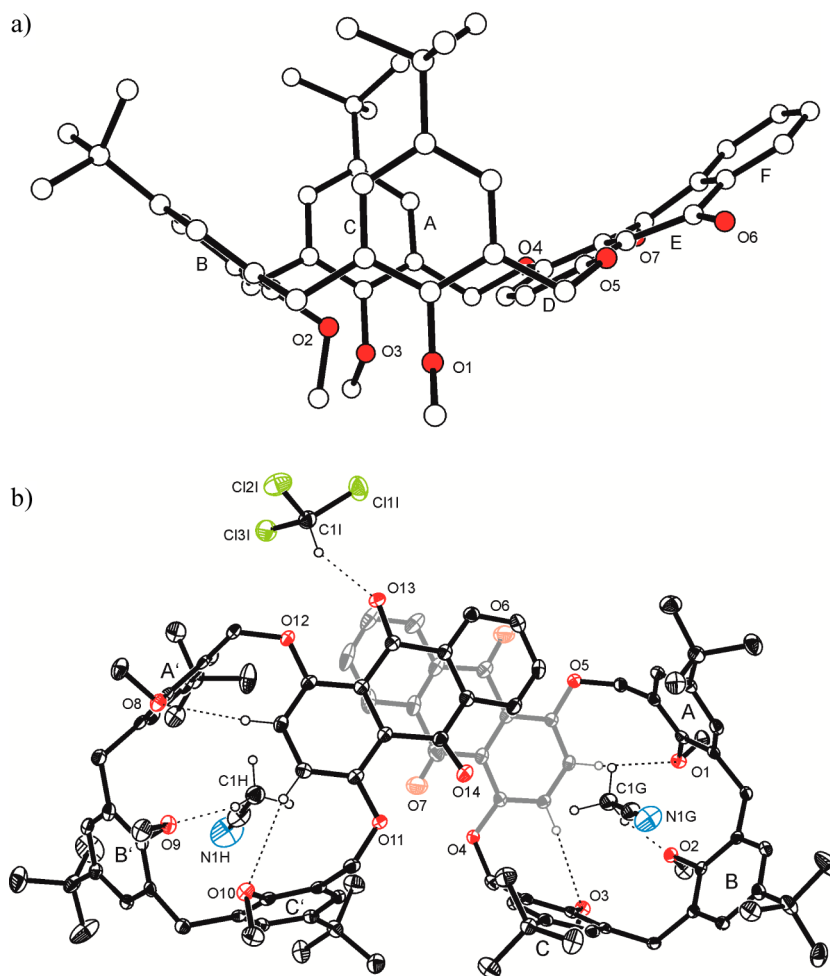


Figure 4. (a) Molecular structure of macrocycle **1** in the 2:2:1 inclusion with acetonitrile and chloroform (**1a**). Only host molecule **1** is displayed; all guest molecules and hydrogen atoms have been omitted for clarity. The disorder of the two *tert*-butyl groups concerned is not displayed. (b) Asymmetric unit of **1a** shown with 50% displacement probability. Only hydrogen atoms involved in intra- and intermolecular contacts are presented.

structure contains a solvent-accessible void of ca. 40 Å³). In both independent hosts of **1a**, *viz.*, molecule **1** and molecule **1'**, the four aromatic units of the macrocycle point in the same direction with corresponding interplanary angles A/C and B/quinizarin of 41.9° (35.9°) and 79.2° (68.5°), respectively (Figure 4a, Table 1). For the centroid-to-centroid distance between the facing arenes, we found 6.83 Å (6.75 Å) and 7.00 Å (7.18 Å), which is considerably larger than for pinched cone calixarenes.²⁷ By way of interest, the bulky quinizarin moiety points toward the cavity. This conformation seems to be stabilized by intramolecular C–H···O contacts [$d(\text{O}\cdots\text{H}) = 2.32\text{--}2.64$ Å] between two aromatic protons of the quinizarin (H37, H38; H87, H88) and the oxygen atoms of two outer methoxy groups (O1, O3; O8, O10). In Figure 4b the trapezoidal form of the cavity becomes obvious, being a result of the ring extension by two oxygen atoms compared to a calix[4]arene. The anthraquinone moieties are both bended by 11°; a phenomenon which is also observed in the structures of quinizarin²⁸ (1.5°), dimethoxyquinizarin²⁹ (22.0°), and quinizarin diacetate³⁰ (8.1°). As it is typical for *tert*-butyl groups, one in each independent host molecule is disordered (SOF = 94.4% and 5.6%).

The acetonitrile molecules within the cavities of molecules **1** and **1'** are tilted by 40.0° and 45.1°, respectively, against the mean plane of the methylene bridges; they are more or less collinear with the aromatic rings B and B'. The ACN methyl groups point into the cavity; each of these *endo* CH₃CN guests is fixed by one C–H··· π contact to the aromatic unit A (A') [$d(\text{centroid}\cdots\text{H}) = 2.88$ and 2.29 Å, respectively] and one C–H···O contact to the methoxy oxygen of ring B (B') [$d(\text{O}\cdots\text{H}) = 2.56$ and 2.57 Å, respectively]. In contrast, the slightly acidic H atom of the *exo* guest chloroform is engaged in a three-centered hydrogen bond.³¹ Additionally, we found a Cl··· π contact³² to the ring B' in molecule **1'** [$d(\text{centroid}\cdots\text{Cl}) = 3.505(2)$ Å].

The two independent molecules **1** and **1'** are connected via their anthraquinone units developing a handshake-like motif. The distance of rings F and F' is 3.411 Å, which suggests aromatic face-to-face contacts. By way of interest, also the quinone moiety is engaged into these interactions. In the overall packing, we found slightly displaced stacks of quinizarin residues units in the direction of the crystallographic *c* axis featuring π ··· π stacking [$d(\text{D}\cdots\text{D}) = 3.454(2)$ Å] (Figure 5). Thereby, two dependent molecules are additionally connected via C–H···O contacts involving methylene and methoxy groups and quinizarin oxygen atoms [$d(\text{centroid}\cdots\text{H}) = 2.53\text{--}2.46$ Å].

When crystallized from acetonitrile, title compound **2** was found to form a 1:3 inclusion compound (**2a**) in the monoclinic space group $P2_1/n$ (Figure 6). One of the guest molecules is accommodated inside the cavity (*endo*) and the two others outside the cavity (*exo*) of the host molecule. Similar to **1a**, the macrocyclic framework adopts a pinched cone conformation with interplanary angles of 33.4° (A/C) and 76.4° (B/quinizarin), respectively (Table 2). The cup-shape of the molecule is stabilized by a strong O–H···O hydrogen bond, which links the phenolic hydroxyl group to one of the neighboring methoxy atoms. Like in **1a**, the sterically demanding anthraquinone moiety is turned toward the cavity (m_{pl}A/m_{pl}Q = 52.3°), and again we found stabilizing C–H···O contacts involving the two methoxy oxygens and quinizarine ring D [$d(\text{O}\cdots\text{H}) = 2.49$ and 2.75 Å, respectively]. The enlarged cavity is able to incorporate one acetonitrile molecule which is fixed by three C–H··· π -interactions³³ to the aromatic rings A, B, and C. Noteworthy, it is tilted by an angle of 48.7° against the mean plane of the four carbon atoms of the methylene bridges and

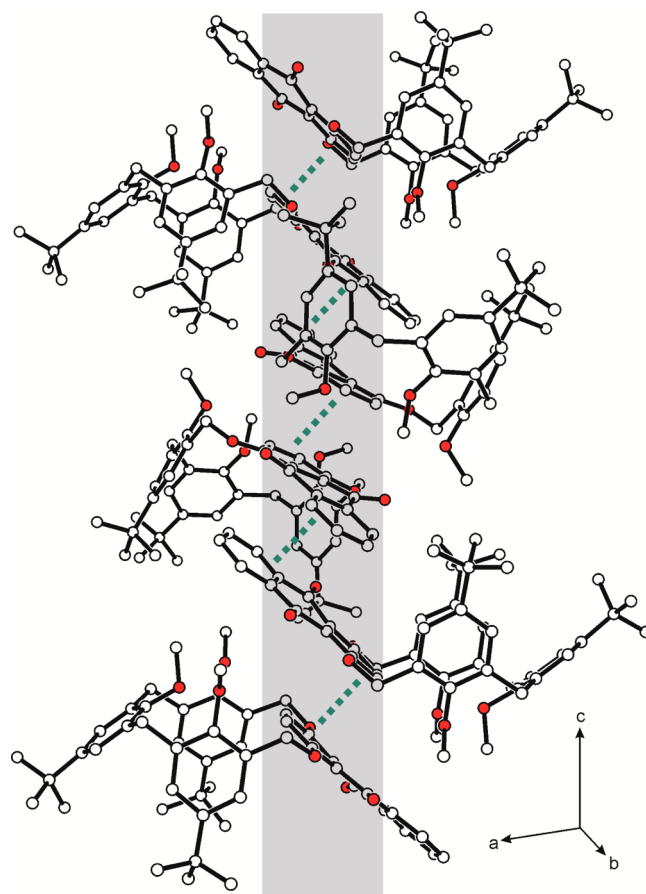


Figure 5. Packing details in the inclusion compound **1a**. The characteristic stacking of the anthraquinone moieties is highlighted in gray. Disordered *tert*-butyl groups, guest molecules, and hydrogen atoms are omitted for clarity.

thereby parallel to the quinizarin unit. Very likely, the reasons for this is a kind of π ··· π stacking, involving quinizarin ring D and the CN triple bond in the acetonitrile [$d = 3.384(2)$ Å]. Additionally, the latter is engaged in an intramolecular C–H··· π contact with a *tert*-butyl H atom H30 ($d = 2.83$ Å).

In the packing of **2a**, two hosts are paired via their quinizarin units developing C–H··· π contacts [$d(\text{H35A}\cdots\text{centroid F}) = 2.93$ Å]. Interestingly, we also observed a close proximity between bridge oxygen O4 and a neighboring quinone unit in ring E [$d = 3.215(2)$ Å] (Figure 7). These contacts resemble charge-transfer-like complexes which are already known from quinones and sulfur.³⁴ Unlike molecule **1**, we observe no continuous aromatic stacking. In the overall packing, all three of the included solvent molecules take part with the *exo*-oriented acetonitrile molecules mediating the connection of the host molecules.

Fluorescence Studies. To extensively characterize the new receptors **1** and **2**, we studied their luminescent behavior in DMSO solution in comparison to that of quinizarin (1,4-dihydroxyanthraquinone) and 1,4-dimethoxyanthraquinone.³⁵ The absorption and fluorescence spectra are presented in Figure 8. Absolute excitation maxima, $\lambda(\text{ex})_{\text{max}}$, absolute emission maxima, $\lambda(\text{em})_{\text{max}}$ and the associated Stokes shifts are summarized in Table 2. The Lambert–Beer law is valid in the entire concentration interval. The fluorescence spectra have been collected at the respective absorption maxima.

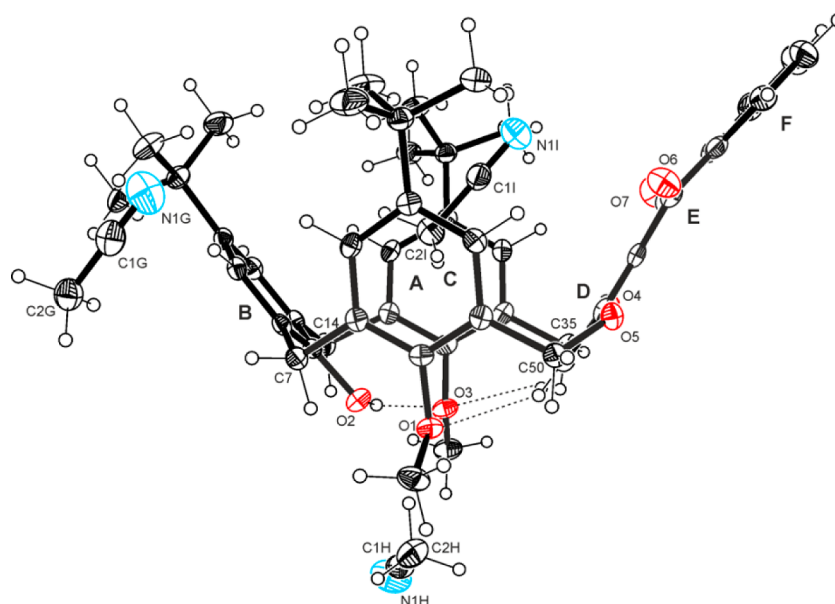


Figure 6. Molecular structure of **2a**, showing 50% probability displacement representation.

Table 2. Fluorescence Data for **1**, **2**, Quinizarin, and 1,4-Dimethoxyanthraquinone in DMSO (20 °C)

compound	1	2	quinizarin	1,4-dimethoxyanthraquinone
$\lambda(\text{ex})_{\text{max}}$ (nm)	423	438	481	426
$\lambda(\text{em})_{\text{max}}$ (nm)	539	548	560	540
Stokes shift (nm)	116	110	79	114

Quinizarin shows a broad absorption maximum at 481 nm, which corresponds to the red color of its solution. Macrocycles **1** and **2** as well as 1,4-dimethoxyanthraquinone experience a hypsochromic shift to 423, 438, and 426 nm, respectively, being in coherence with their yellow solutions. The color change is obviously a result of the altered electronic situation connected with the etherification of the hydroxyl groups of the quinizarin. The fluorescence maxima for **1** and **2** have been determined with 539 and 548 nm, which is slightly lower than for quinizarin (560 nm) and similar to 1,4-dimethoxyanthraquinone (540 nm). The resulting Stokes shifts are considerably higher for the macrocycles and 1,4-dimethoxyanthraquinone than for quinizarin. By way of interest, the excitation and emission spectra of quinizarin

develop a rather pronounced plateau; this may result from a higher aggregation of the molecules.

CONCLUSION

Two unprecedented cyclophanes (**1** and **2**) with intrinsic fluorescence have been synthesized from putative linear trimers and quinizarin applying the principle of Ziegler and Ruggli.²² The constitution of the molecules is related to that of methylated calixarenes, though we observed a different conformational behavior. In general, trimethoxy cycle **1** shows a flexibility higher than that of the monophenolic cycle **2**, which is stabilized by a strong hydrogen bond. For each of the title compounds, temperature-dependent ¹H NMR spectroscopy revealed a typical sharpening of the methylene resonances and a conformational stabilization with decreasing temperatures. These findings justify the assumption of “cone” conformations with all four aromatic units pointing in one direction for both cycles. This hypothesis is supported by respective shifts of the methylene carbons in the ¹³C NMR spectra and pertinent NOEs. The cup-shape of both title molecules has also been confirmed by molecular modeling and X-ray crystallography. It seems opportune to assume that C–H...O contacts between the methoxy oxygen atoms and the

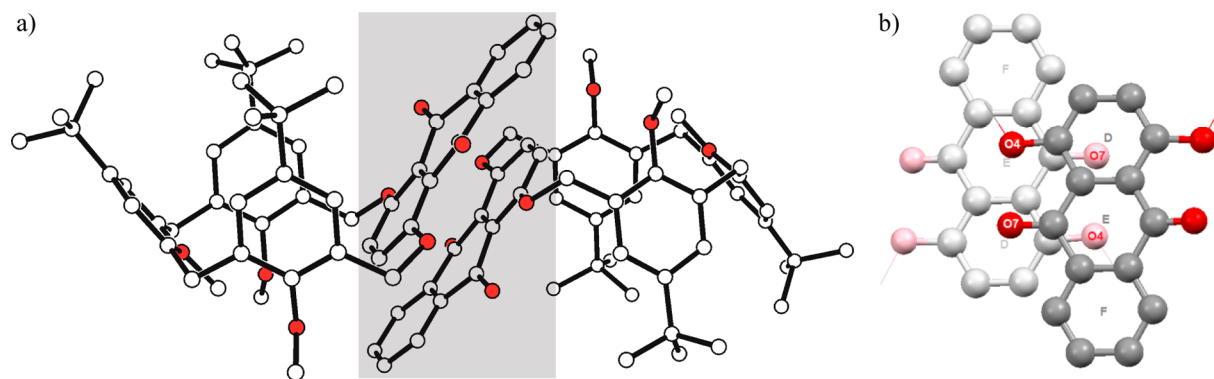


Figure 7. (a) Dimer formation in the packing of **2** in its 1:3 acetonitrile inclusion compound (**2a**). Guest molecules and hydrogen atoms are left out for clarity. (b) The two paired anthraquinone units in **2a** resemble a charge-transfer complex.

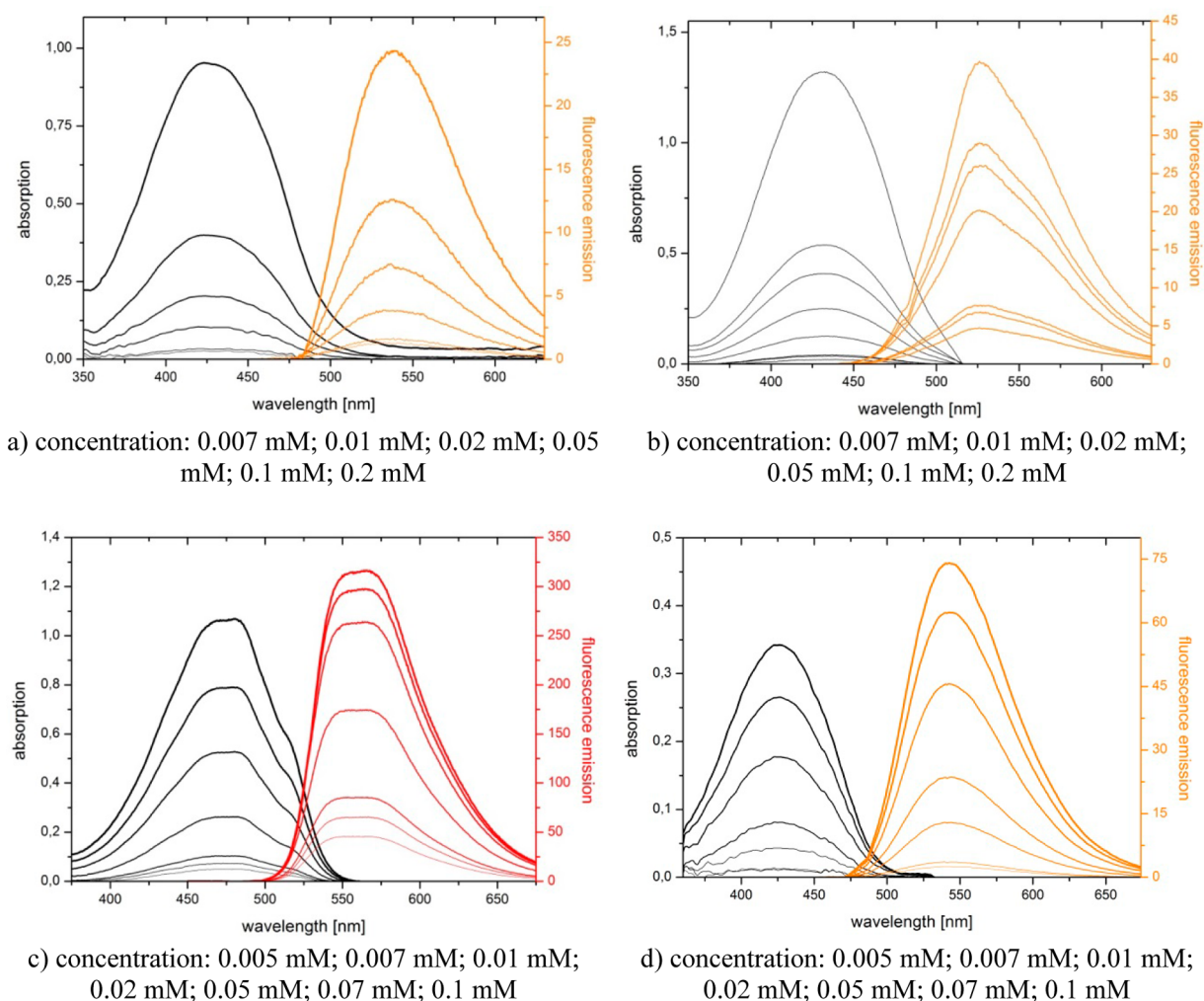


Figure 8. Excitation and fluorescence emission spectra of macrocycles **1** (a), **2** (b), quinizarin (c), and 1,4-dimethoxyanthraquinone (d) at different concentrations in DMSO.

quinizarin fulfill here the function of the strong O–H...O bonds found in calixarenes to stabilize the cone conformation. Moreover, fast exchange processes in the NMR spectra of **1** and **2** suggest two rather similar cone forms for each cycle similar to pinched cone calixarenes.

As demonstrated by excitation and fluorescence emission spectra, the incorporation of an anthraquinone unit into a cyclophane does not change its luminescent behavior. The additional plane, electron-rich fluorophore in **1** and **2** allows additional interactions toward potential guest molecules as shown for acetonitrile complexes. We found a better fit between host and guest with more stabilizing C–H...O and C–H... π contacts in comparison to the somewhat smaller calix[4]arenes. This is especially true for cycle **2**, where all three hydrogen atoms of the acetonitrile molecule are involved in the complexation. By regarding acetonitrile as a simple model of methylamines, these findings are encouraging the further development of this promising new class of macrocycles. Our next step in this respect will be the introduction of hydrophilic groups to the molecules resulting in water-soluble receptors.

EXPERIMENTAL SECTION

Materials and Methods. Melting points have been determined on a microscope heating stage and are uncorrected. IR spectra were measured as KBr pellets and with the ATR method. The UV/vis and

fluorescence measurements have been carried out using quartz cuvettes (10 × 10 mm) and diluting the respective stock solutions in DMSO (**1**: $c = 1.3$ mmol/L; **2**: $c = 1.2$ mmol/L; quinizarin: $c = 1.2$ mmol/L; 1,4-dimethoxyanthraquinone: $c = 1.2$ mmol/L) to the concentrations specified. NMR spectra were recorded at 500.1 (^1H NMR) and 125.7 MHz (^{13}C NMR), respectively, with sample temperatures regulated at 293 K, unless otherwise stated. Spectra have been assigned using COSY, DEPT-135, HSQC, and HMBC. Chemical shifts δ are reported in parts per million relative to the internal reference TMS. Multiplicity is abbreviated as follows: s (singlet), d (doublet), t (triplet), and m (multiplet). Analytical TLC was performed on precoated silica gel plates (60 F₂₅₄). The reagents and solvents were used as purchased from the chemical suppliers, with the exception of those for cyclization reaction (dried dynamically over molecular sieves, 3 Å). The trimers **3**¹⁶ and **6**¹⁵ as well as quinizarin³⁶ were prepared according to literature procedures. 1,4-Dimethoxyanthraquinone is commercially available. For the energy minimizations, we used the program MacroModel V.9.8 (OPLS_2001 force field, MCMM, 1000 steps).

5-tert-Butyl-1,3-bis(5-tert-butyl-2-methoxybenzyl)-2-methoxybenzene (4).³⁷ The phenolic trimer **3** (5.50 g, 11.6 mmol) was dissolved in THF (130 mL) and DMF (10 mL). Subsequently, NaH (60% in paraffin, 3.00 g, 127.6 mmol) and MeI (8.7 mL, 139.50 mmol) were added carefully. Heating under reflux for 4 h produced a white precipitate. Subsequently, the solvent was evaporated and the residue taken up in chloroform and water. The organic phase was separated and the solvent removed almost completely. The white precipitate of **4** formed after addition of MeOH was filtered, washed first with MeOH and then with ether, and dried afterward. Yield: 5.85 g (97%). Mp 138–

139 °C (lit.³⁸ 140–141 °C). ¹H NMR (CDCl₃): 1.17 (s, 9H, C(CH₃)); 1.22 (s, 18H, C(CH₃)); 3.61 (s, 3H, ArOCH₃); 3.81 (s, 6H, ArOCH₃); 4.03 (s, 4H, ArCH₂Ar); 6.80 (d, 2H, ArCH, ³J_{HH} = 8.5 Hz); 6.98 (s, 2H, ArCH); 7.06 (d, 2H, ArCH, ⁴J_{HH} = 2.5 Hz); 7.18 (dd, 2H, ArCH, ³J_{HH} = 8.5 Hz, ⁴J_{HH} = 2.5 Hz); ¹³C NMR (CDCl₃): 30.0 (CH₂), 31.4, 31.5 (C(CH₃)); 34.0, 34.2 (C(CH₃)); 55.4, 61.0 (ArOCH₃); 109.7, 123.3, 126.1, 127.7, 129.1, 132.5, 142.8, 145.9, 154.9, 155.4 (ArC). *m/z* (SI): Calcd: 516.36, found: 555.26 (M + K⁺) IR (cm⁻¹): 2951, 2901, 2865, 2836, 1609, 1505, 1461, 1245, 1135, 1011, 816. Elemental analysis calculated for C₃₅H₄₈O₃: C, 81.35%; H, 9.36%. Found: C, 81.72%; H, 9.82%.

1,3-Bis[3-(bromomethyl)-5-(tert-butyl)-2-methoxyphenyl]-methyl]-5-(tert-butyl)-2-hydroxybenzene (5). Methyl ether 4 (3.00 g, 5.8 mmol), paraformaldehyde (0.42 g, 14.0 mmol), and glacial acetic acid (40 mL) were stirred for 1 h at 70 °C in a bomb tube. To the white suspension were added zinc bromide (1.30 g, 5.8 mmol) and hydrogen bromide (33% in glacial acetic acid, 5.8 mL), and stirring was continued for 5 h at 70 °C. After cooling, the clear brown solution was poured into water, whereupon a white cloudy suspension appeared. After extraction with CH₂Cl₂, the organic phase was dried over MgSO₄ and the solvent was evaporated under reduced pressure. The resulting brown oil was column chromatographed on SiO₂ (eluent: *n*-hexane/ethyl acetate, 14:1) to yield 0.38 g (9%) of a beige solid. Mp 158–160 °C. TLC: R_f = 0.19 (SiO₂; *n*-hexane/chloroform, 1:1). ¹H NMR (CDCl₃): 1.20 (s, 27H, C(CH₃)); 3.93 (s, 4H, ArCH₂Ar); 3.95 (s, 6H, ArOCH₃); 4.58 (s, 4H, ArCH₂OAr); 6.98 (s, 2H, ArCH); 7.15 (d, 2H, ArCH, ⁴J_{HH} = 2.5 Hz); 7.24 (d, 2H, ArCH, ⁴J_{HH} = 2.5 Hz); 7.34 (s, 1H, ArOH); ¹³C NMR (CDCl₃): 28.8, 31.0 (CH₂); 31.3, 31.5 (C(CH₃)); 34.0, 34.3 (C(CH₃)); 62.2 (ArOCH₃); 125.6, 126.5, 126.7, 128.9, 130.3, 133.3, 142.7, 147.8, 149.9, 153.2 (ArC). *m/z* (APCI): Calcd: 688.19, found: 687.50 [M⁻]. IR (cm⁻¹): 3374, 2956, 2901, 2866, 1600, 1481, 1434, 1218, 1203, 988, 880, 751. Elemental analysis calculated for C₃₆H₄₈Br₂O₃·2H₂O: C, 59.67%; H, 7.23%. Found: C, 59.17%; H, 7.06%. Additionally to **5**, we isolated 0.15 g (4% yield) of the fully methylated trimer **6**.

1,3-Bis[3-(bromomethyl)-5-(tert-butyl)-2-methoxyphenyl]-methyl]-5-(tert-butyl)-2-methoxybenzene (6). Under an argon atmosphere, methyl ether 4 (4.75 g, 9.2 mmol), dissolved in TFA (20 mL), was treated with bromomethyl methyl ether (1.0 mL, 1.53 g, 12.3 mmol). After 24 h, the brownish solution was quenched with water, followed by extraction with CHCl₃. The organic phase was dried over MgSO₄ and the solvent was evaporated under reduced pressure. The resulting green oil was column chromatographed on SiO₂ (eluent: *n*-hexane/chloroform, 1:1 → 1:2) to yield 0.70 g (11%) of a colorless oil, which crystallized later. Mp 120–122 °C. TLC: R_f = 0.25 (SiO₂; *n*-hexane/chloroform, 1:1). ¹H NMR (CDCl₃): 1.16 (s, 9H, C(CH₃)); 1.21 (s, 18H, C(CH₃)); 3.59 (s, 3H, ArOCH₃); 3.84 (s, 6H, ArOCH₃); 4.08 (s, 4H, ArCH₂Ar); 4.61 (s, 4H, ArCH₂Br); 6.94 (s, 2H, ArCH); 7.02 (d, 2H, ArCH, ⁴J_{HH} = 2.5 Hz); 7.25 (d, 2H, ArCH, ⁴J_{HH} = 2.6 Hz); ¹³C NMR (CDCl₃): 29.1, 29.9 (CH₂); 31.3, 31.4 (C(CH₃)); 34.2, 34.3 (C(CH₃)); 60.8, 61.3 (ArOCH₃); 126.2, 126.2, 128.9, 130.3, 132.5, 133.9, 146.5, 147.0, 154.5, 154.7 (ArC). *m/z* (SI): Calcd: 702.21, found: 725.30 [M + Na⁺], 741.3 [M + K⁺]. IR (cm⁻¹): 3672, 2955, 2826, 1583, 1480, 1220, 1203, 1006, 882. Elemental analysis calculated for C₃₆H₄₈Br₂O₃·H₂O: C, 62.45%; H, 7.22%. Found: C, 62.13%; H, 7.41%.

General Synthetic Procedures for Macrocycles 1 and 2. Under an argon atmosphere, the respective trimer **5** or **6** and quinzarin, each dissolved in dry acetone (250 mL per 0.55 mmol of the trimer), are slowly dropped into a refluxing suspension of K₂CO₃ (4 equiv) in dry acetone (100 mL per 0.55 mmol trimer) using a high-dilution apparatus.²¹ The color of the reaction mixture changes from dark blue to dark green. After 48 h of refluxing, solid components are removed by filtration. The solvent was evaporated, and the resulting reddish brown oil was column chromatographed on SiO₂ (eluent for **1**: chloroform/ethyl acetate, 24:1; eluent for **2**: *n*-hexane/ethyl acetate, 2:1) to yield macrocycles **1** and **2** as orange solids.

2,10-Dioxa-4¹,6⁴,8⁴-tri-tert-butyl-4¹,6¹,8¹-trimethoxy-1(1,4)-anthraquinona-4,6,8(2,6)-tribenzenacyclodecapane (1). Yield 435 mg (58%). Mp 280–282 °C. TLC: R_f = 0.44 (SiO₂; chloroform/ethyl acetate, 24:1). ¹H NMR (CDCl₃): 0.86 (s, 18H, C(CH₃)); 1.38 (s,

9H, C(CH₃)); 3.50 (s, 2H, ArCH₂Ar);³⁹ 3.63 (s, 3H, ArOCH₃); 3.72 (s, 6H, ArOCH₃); 4.31 (s, 2H, ArCH₂Ar);³⁹ 5.37 (s, 4H, ArCH₂OAr); 6.78 (s, 2H, 37-, 38-ArCH); 6.81 (s, 2H, 5-, 17-ArCH); 7.11 (d, 2H, 3-, 19-ArCH, ⁴J_{HH} = 1.5 Hz); 7.25 (s, 2H, 10-, 12-ArCH); 7.69 (m, 2H, 44-, 45-ArCH); 8.18 (m, 2H, 43-, 46-ArCH); ¹³C NMR (CDCl₃): 31.0 (C(CH₃)); 31.5 (CH₂); 31.6 (C(CH₃)); 33.9, 34.2 (C(CH₃)); 60.3, 62.3 (ArOCH₃); 64.4 (OCH₂); 122.7 (40-, 49-ArC); 123.0 (37-, 38-ArC); 124.0 (3-, 19-ArC); 126.3 (43-, 46-ArC); 126.8 (10-, 12-ArC); 127.0 (5-, 17-ArC); 128.3 (2-, 20-ArC); 132.9 (9-, 13-ArC); 133.0 (44-, 45-ArC); 134.3 (42-, 47-ArC); 134.5 (6-, 16-ArC); 145.8 (11-ArC); 146.7 (4-, 18-ArC); 151.9 (36-, 39-ArC); 153.8 (1-, 15-ArC); 155.0 (8-ArC); 183.4 (C=O). *m/z* (SI): Calcd: 780.40, found: 803.37 (M + Na⁺). IR (cm⁻¹): 3442, 2960, 2905, 2870, 2826, 1668, 1595, 1567, 1483, 1465, 1255, 1238, 1216, 1014, 727. Elemental analysis calculated for C₅₁H₅₆O₇·1/2 CH₃COOCH₂CH₃: C, 77.16%; H, 7.33%. Found: C, 77.01%; H, 7.36%.

4¹,8¹-Dimethoxy-2,10-dioxa-6¹-hydroxy-4⁴,6⁴,8⁴-tri-tert-butyl-1(1,4)-anthraquinona-4,6,8(2,6)-tribenzenacyclodecapane (2). Yield: 75 mg (18%). Mp 234–236 °C. TLC: R_f = 0.22 (SiO₂; *n*-hexane/ethyl acetate, 2:1). ¹H NMR (CDCl₃): 0.88 (s, 18H, C(CH₃)); 1.34 (s, 9H, C(CH₃)); 3.44 (br s, 2H, ArCH₂Ar); 3.91 (s, 6H, ArOCH₃); 4.30 (br s, 2H, ArCH₂Ar); 5.38 (br s, 2H, ArCH₂OAr); 5.45 (br s, 2H, ArCH₂OAr); 6.62 (s, 1H, ArOH); 6.89 (d, 2H, 5-, 17-ArCH, ⁴J_{HH} = 2.5 Hz); 7.13 (s, 2H, 37-, 38-ArCH); 7.19 (s, 2H, 10-, 12-ArCH); 7.23 (d, 2H, 3-, 19-ArCH, ⁴J_{HH} = 2.5 Hz); 7.68 (m, 2H, 44-, 45-ArCH); 8.15 (m, 2H, 43-, 46-ArCH); ¹³C NMR (CDCl₃): 30.3 (CH₂); 30.9, 31.7 (C(CH₃)); 33.9, 34.0 (C(CH₃)); 63.3 (OCH₂); 63.8 (ArOCH₃); 121.7 (37-, 38-ArC); 122.7 (40-, 49-ArC); 125.0 (3-, 19-ArC); 126.2 (44-, 45-ArC); 126.4 (10-, 12-ArC); 126.5 (9-, 13-ArC); 127.1 (5-, 17-ArC); 128.2 (2-, 20-ArC); 132.0 (6-, 16-ArC); 132.9 (43-, 46-ArC); 134.5 (42-, 47-ArC); 142.1 (11-ArC); 147.8 (21-, 29-ArC); 150.0 (8-ArC); 151.5 (36-, 39-ArC); 152.5 (1-, 15-ArC); 183.3 (C=O). *m/z* (SI): Calcd: 766.39, found: 789.40 (M + Na⁺). IR (cm⁻¹): 2953, 1667, 1635, 1591, 1568, 1483, 1237, 1210, 981, 795, 726. Elemental analysis calculated for C₅₀H₅₄O₇·1/2 CH₃COOCH₂CH₃: C, 77.01%; H, 7.21%. Found: C, 76.91%; H, 7.60%.

X-ray Structure Determination. Crystals of compounds **1a**, **2a**, and **4** suitable for X-ray diffraction have been obtained by slow evaporation of the respective solution (**1** in acetonitrile/chloroform (1:1), **2** in acetonitrile and **4** in ethyl acetate). The intensity data were collected at 100 K on a Bruker Kappa diffractometer equipped with an APEX II CCD area detector and graphite-monochromatized Mo K α radiation (λ = 0.71073 Å) employing φ and ω scan modes. The data were corrected for Lorentz and polarization effects. Semiempirical absorption correction was applied using the SADABS program.⁴⁰ The SAINT program⁴⁰ was used for the integration of the diffraction profiles. The crystal structures were solved by direct methods using SHELXS-97⁴¹ and refined by full-matrix least-squares refinement against *F*² using SHELXL-97.⁴¹ All non-hydrogen atoms were refined anisotropically. Hydrogen atoms were positioned geometrically and allowed to ride on their parent atoms. Geometrical calculations were performed using PLATON, and molecular graphics were generated using SHELXTL.⁴¹ The crystallographic data for the structures in this paper have been deposited with the Cambridge Crystallographic Data Centre; CCDC numbers: 1042786 (**1**), 1042787 (**2**), and 1042788 (**4**).

■ ASSOCIATED CONTENT

● Supporting Information

Energy-minimized structures of **1** and **2**. ¹H and ¹³C NMR spectra of compounds **1**, **2**, **4**, **5**, and **6**; NOESY spectra of **1** and **2**. Selected details of the data collection; table of distances and angles of inter- and intramolecular contacts in the structures of **1a**, **2a**, and **4**; description of the X-ray structure of **4**. X-ray crystallographic data files (CIF) for **1**, **2**, and **4**. The Supporting Information is available free of charge on the ACS Publications website at DOI: 10.1021/acs.joc.5b00223.

AUTHOR INFORMATION

Corresponding Author

*Tel: +49 3731 392390. E-mail: Tobias.Gruher@chemie.tu-freiberg.de.

Notes

The authors declare no competing financial interest.

ACKNOWLEDGMENTS

Financial support from 'Fonds der Chemischen Industrie' and the Institute of Organic Chemistry, University of Freiberg, is gratefully acknowledged. Furthermore, we thank M. Stapf for his helpful advice.

REFERENCES

- (1) Valeur, B. *Molecular Fluorescence. Principles and Applications*, 2nd ed.; Wiley-VCH: Weinheim, 2013.
- (2) Parkesh, R.; Veale, E. B.; Gunnlaugsson, T. *Chemosensors*; Wang, B.; Slyn, E. V., Eds.; Wiley: New York, 2011; pp 229–252.
- (3) (a) Azadbakht, R.; Khanabadi, J. *Spectrochim. Acta* **2014**, *A124*, 249–255. (b) Nativi, C.; Francesconi, O.; Gabrielli, G.; De Simone, L.; Turchetti, B.; Mello, T.; Di Cesare Manelli, L.; Ghelardini, C.; Buzzini, P.; Roelens, S. *Chem.—Eur. J.* **2012**, *18*, 5064–5072. (c) Alfonso, I.; Burguete, M. I.; Galindo, F.; Luis, S. V.; Vigara, L. *J. Org. Chem.* **2009**, *74*, 6130–6142.
- (4) (a) Li, Z.; Sei, Y.; Akita, M.; Yoshizawa, M. *Chem.—Asian J.* **2014**, *9*, 1016–1019. (b) Ahmed, N.; Shirinfar, B.; Youn, I. S.; Yousuf, M.; Kim, K. S. *Org. Biomol. Chem.* **2013**, *11*, 6407–6413. (c) Ghosh, K.; Sarkar, A. R. *Tetrahedron Lett.* **2009**, *50*, 85–88.
- (5) (a) Halling, M. D.; Unikel, K. S.; Bodwell, G. J.; Grant, D. M.; Pugmire, R. J. *J. Phys. Chem. A* **2012**, *116*, 5193–5198. (b) Nandaluru, P. R.; Dongare, P.; Kraml, C. M.; Pascal, R. A., Jr.; Dawe, L. N.; Thompson, D. W.; Bodwell, G. J. *Chem. Commun.* **2012**, *48*, 7747–7749. (c) Franz, D.; Robbins, S. J.; Boeré, R. T.; Dibble, P. W. *J. Org. Chem.* **2009**, *74*, 7544–7547. (d) Tsuge, A.; Otsuka, M.; Moriguchi, T.; Sakata, K. *Org. Biomol. Chem.* **2005**, *3*, 3590–3593. (e) Abe, H.; Mawatari, Y.; Teraoka, H.; Fujimoto, K.; Inouye, M. *J. Org. Chem.* **2004**, *69*, 495–504.
- (6) (a) Rajakumar, P.; Anandhan, R. *Synth. Commun.* **2013**, *43*, 882–892. (b) Rajakumar, P.; Kanagalatha, R. *Tetrahedron Lett.* **2007**, *48*, 2761–2764. (c) Lukyanenko, N. G.; Lyapunov, A. Y.; Kirichenko, T. I.; Botoshansky, M. M.; Simonov, Y. A.; Fonari, M. S. *Tetrahedron Lett.* **2005**, *46*, 2109–2112. (d) Matsumoto, K.; Minami, H.; Kawase, T.; Oda, M. *Org. Biomol. Chem.* **2004**, *2*, 2323–2326.
- (7) (a) Chu, M.; Scioneaux, A. N.; Hartley, C. S. *J. Org. Chem.* **2014**, *79*, 9009–9017. (b) Balakrishnan, K.; Datar, A.; Zhang, W.; Yang, X.; Naddo, T.; Huang, J.; Zuo, J.; Yen, M.; Moore, J. S.; Zang, L. *J. Am. Chem. Soc.* **2006**, *128*, 6576–6577. (c) Yasuhide, I.; Takahiro, M.; Noboru, O.; Hidemitsu, U.; Atsuhiko, O. *Angew. Chem., Int. Ed.* **2005**, *44*, 1856–1860.
- (8) Gleiter, R.; Hopf, H., Eds. *Modern Cyclophane Chemistry*; Wiley: Weinheim, 2004.
- (9) (a) Gutsche, C. D. *Calixarenes*; The Royal Society of Chemistry: Cambridge, UK, 2008. (b) Vicens, J.; Harrowfield, J. *Calixarenes in the Nanoworld*; Springer-Verlag: Dordrecht, 2007. (c) Asfari, M. Z.; Böhmer, V.; Harrowfield, J.; Vicens, J. *Calixarenes 2001*; Kluwer Academic: Dordrecht, 2001. (d) Mandolini, L.; Ungaro, R. *Calixarenes in Action*; Imperial College Press: London, 2000.
- (10) Steed, J. W.; Atwood, J. L. *Supramolecular Chemistry*, 2nd ed.; John Wiley & Sons: Chichester, 2009.
- (11) (a) Song, M.; Sun, Z.; Han, C.; Tian, D.; Li, H.; Kim, J. S. *Chem.—Asian J.* **2014**, *9*, 2344–2357. (b) Ocak, U.; Ocak, M.; Bartsch, R. A. *Inorg. Chim. Acta* **2012**, *381*, 44–57. (c) Sharma, K.; Cragg, P. J. *Chem. Sensors* **2011**, *1*, 9/1–9/18. (d) Fischer, C.; Gruher, T.; Seichter, W.; Weber, E. *Org. Biomol. Chem.* **2011**, *9*, 4347–4352. (e) Talanova, G. G.; Talanov, V. S. *Supramol. Chem.* **2010**, *22*, 838–852. (f) Chawla, H. M.; Pant, N.; Kumar, S.; Kumar, N.; Black, D. StC. Calixarene-based materials for Chemical Sensors. In *Chemical Sensors: Fundamentals of*

Sensing Materials; Korotcenkov, G., Ed.; Momentum Press: New York, 2010; Vol. 3. (g) Lo, P. K.; Wong, M. S. *Sensors* **2008**, *8*, 5313–5335.

(12) Georghiou, P. E.; Li, Z.; Ashram, M.; Chowdhury, S.; Mizyed, S.; Tran, A. H.; Al-Saraierh, H.; Miller, D. O. *Synlett* **2005**, *6*, 879–891.

(13) (a) Moreno-Corral, R.; Lara, K. O. *Supramol. Chem.* **2008**, *20*, 427–435. (b) Gu, S.-J.; Qin, D.-B.; Jin, L.-H. *Chin. J. Struct. Chem.* **2008**, *27*, 1035–1038. (c) Kitamura, C.; Fujimoto, J.; Kawatsuki, N.; Yoneda, A. *Heterocycles* **2006**, *68*, 2171–2175. (d) Haeg, M. E.; Whitlock, B. J.; Whitlock, H. W., Jr. *J. Am. Chem. Soc.* **1989**, *111*, 692–696. (e) Buhleier, E.; Vögtle, F. *Chem. Ber.* **1978**, *111*, 2729–2731.

(14) Bhattacharya, D.; Sathiyendiran, M.; Wu, J.-Y.; Chang, C.-H.; Huang, S.-C.; Zeng, Y.-L.; Lin, C.-Y.; Thanasekaran, P.; Lin, B.-C.; Hsu, C.-P.; Lee, G. H.; Peng, S. M.; Lu, K. L. *Inorg. Chem.* **2010**, *49*, 10264–10272.

(15) (a) Lin, C.-X.; Kong, X.-F.; Li, Q.-S.; Zhang, Z.-Z.; Yuan, Y.-F.; Xu, F.-B. *CrystEngComm* **2013**, *13*, 6948–6962. (b) Qin, D.-B.; Xu, F.-B.; Li, Q.-S.; Song, H.-B.; Zhang, Z.-Z. *Synlett* **2005**, *19*, 2987–2989.

(16) Dhawan, B.; Gutsche, C. D. *J. Org. Chem.* **1983**, *48*, 1536–1539.

(17) Li, H.; Homan, E. A.; Lampkins, A. J.; Ghiviriga, L.; Castellano, R. K. *Org. Lett.* **2005**, *7*, 443–446.

(18) (a) Kämmerer, H.; Schweikert, H.; Haub, H.-G. *Makromol. Chem.* **1963**, *67*, 173–181. (b) Kämmerer, H.; Gros, G.; Schweikert, H. *Makromol. Chem.* **1971**, *143*, 135–152.

(19) (a) Hornung, E. *J. Org. Chem.* **1945**, *10*, 263–266. (b) Pickholtz, Y.; Sasson, Y.; Blum, J. *Tetrahedron Lett.* **1974**, *14*, 1263–1266. (c) Aizenshtat, Z.; Hausmann, M.; Pickholtz, Y.; Tal, D.; Blum, J. *J. Org. Chem.* **1977**, *42*, 2386–2394.

(20) We used 4-*tert*-butyl-2,6-bis[(5-*tert*-butyl-2-methoxyphenyl)methyl]phenol as the monophenolic trimer. The pK_a have been calculated using Advanced Chemistry Development (ACD/Laboratories) Software V11.02 (1994–2014 ACD/Laboratories) as employed in SciFinder.

(21) Vögtle, F. *Chem.-Ztg.* **1972**, *96*, 396–403.

(22) (a) Ziegler, K.; Eberle, H.; Ohlinger, H. *Justus Liebigs Ann. Chem.* **1933**, *504*, 94–130. (b) Ziegler, K.; Aurnhammer, R. *Justus Liebigs Ann. Chem.* **1934**, *513*, 43–64. (c) Knops, P.; Sendhoff, N.; Meikelburger, H.-B.; Vögtle, F. *Top. Curr. Chem.* **1991**, *161*, 1–36.

(23) (a) Kuno, L.; Biali, S. E. *J. Org. Chem.* **2011**, *76*, 3664–3675. (b) Gruner, M.; Fischer, C.; Gruher, T.; Weber, E. *Supramol. Chem.* **2010**, *22*, 256–266. (c) Choe, J.-I.; Lee, S. H.; Oh, D.-S. *Bull. Korean Chem. Soc.* **2004**, *25*, 55–58.

(24) Jaime, C.; de Mendoza, J.; Prados, P.; Nieto, P. M.; Sánchez, C. J. *Org. Chem.* **1991**, *56*, 3372–3376.

(25) Gutsche, C. D.; Bauer, L. J. *Tetrahedron Lett.* **1981**, *22*, 4763–4766.

(26) Gruher, T.; Gruner, M.; Fischer, C.; Seichter, W.; Bombicz, P.; Weber, E. *New J. Chem.* **2010**, *34*, 250–259.

(27) Gruher, T.; Bombicz, P.; Seichter, W.; Weber, E. *J. Struct. Chem.* **2009**, *50*, 522–531.

(28) (a) Nigam, G. D.; Deppisch, B. Z. *Kristallogr.* **1980**, *151*, 185–191. (b) Swaminathan, S.; Nigam, G. D. *Curr. Sci.* **1967**, *36*, 541. (c) Murty, B. V. R. Z. *Kristallogr.* **1959**, *111*, 238–239.

(29) Cao, L.-P.; Wang, Y.-Z.; Gao, M.; Zhou, B.-H. *Acta Crystallogr.* **2007**, *E63*, o1876–o1877.

(30) Zhang, J.-J.; Yina, C.-X.; Huob, F.-J. *Acta Crystallogr.* **2013**, *E69*, o788.

(31) Jeffrey, G. A. *An introduction to hydrogen bonding*; Oxford University Press: Oxford, UK, 1997.

(32) (a) Saraogi, I.; Vijay, V. G.; Das, S.; Sekar, K.; Guru Row, T. N. *Cryst. Eng.* **2003**, *6*, 69–77. (b) Yumi, N. I.; Inoue, Y.; Nakanishi, I.; Kitaura, K. *Protein Sci.* **2008**, *17*, 1129–1137.

(33) Nishio, M.; Umezawa, Y.; Honda, K.; Tsuboyama, S.; Suezawa, H. *CrystEngComm* **2009**, *11*, 1757–1788.

(34) Aly, A. A.; Elkanzi, N. A. A.; Brown, A. B. *Phosphorus Sulfur Silicon Relat. Elem.* **2014**, *189*, 440–452.

(35) For the respective spectra in methylcyclohexane, see: Shcheglova, N. A.; Shigorin, D. N.; Sergeev, A. M. *Zh. Fiz. Khim.* **1979**, *53*, 1749–1752.

- (36) Gattermann, L.; Wieland, H.; Wieland, T. *Die Praxis des Organischen Chemikers*, 43rd ed.; de Gruyter: Berlin, 1982.
- (37) Similar to: Yamagishi, T.; Enoki, M.; Inui, M.; Furukawa, H.; Nakamoto, Y.; Ishida, S. *J. Polym. Sci., Part A: Polym. Chem.* **1993**, *31*, 675–682.
- (38) Zinke, A.; Ott, R.; Garrana, F. H. *Monatsh. Chem.* **1958**, *89*, 135–142.
- (39) The respective signal is not visible at room temperature. We display here the chemical shift at $-35\text{ }^{\circ}\text{C}$.
- (40) Bruker, SAINT, SADABS, AXS Inc., Madison, WI, 2007.
- (41) Sheldrick, G. M. *Acta Crystallogr.* **2008**, *A64*, 112–122.